An Improved Air-Light Estimation Scheme for Single Haze Images Using Color Constancy Prior

Sidharth Gautam , *Member, IEEE*, Tapan Kumar Gandhi , and B.K. Panigrahi , *Senior Member, IEEE*

Abstract—Hazy environment attenuates the scene radiance and causes difficulty in distinguishing the color and texture of the scene. A crucial step in dehazing is the recovery of the global air-light vector. Traditional methods usually interpret the RGB value of the brightest region in haze images as the air-light. In this letter, a new prior called 'color constancy prior' has been proposed to improve the robustness of air-light estimation when varicolored illumination exists. The prior utilizes the statistical observation that distant scenery objects become the most haze-opaque due to the pixel escalation towards the higher intensity side. The comparative evaluation on a variety of haze images manifests that the proposed prior perform better than existing air-light recovery methods and can be used for subsequent dehazing applications.

Index Terms—Air-light estimation, dehazing.

I. Introduction

THE atmospheric light absorbed and scattered by haze or smoky environment obscure the scene visibility due to the addition of an ambient light layer called air-light. The ambient air-light layer fades the true colors by adding whiteness in the scene and cause a reduction in overall image clarity. Based on this observation, the influences of air-light on natural images can be described using a haze model [1]-[2]:

$$I(\mathbf{x}) = J(\mathbf{x})T(\mathbf{x}) + A_\infty(1 - T(\mathbf{x})) \tag{1}$$

$$T(\mathbf{x}) = e^{-\beta d(\mathbf{x})} \tag{2}$$

where I and $J \in \Re^{M \times N \times 3}$ are the haze and the haze-free image, $\mathbf{x} = f(x, y) \in \Re^2$ is the pixel coordinates, $T \in \Re^{M \times N}$ is the transmission-map exponentially related to the scattering coefficient ($\beta \in \Re \mid 0 < \beta \le n$) and scene depth-map $d(\mathbf{x}) \in \Re^{M \times N}$, $A_\infty = [A_\infty^r, A_\infty^g, A_\infty^b] \in \Re^3$ is the RGB vector representing the intensity of global air-light. In Eq. (1), term $A_\infty(1 - T(\mathbf{x}))$ is called the air-light layer, responsible for adding whiteness or air-light color to the scene $J(\mathbf{x})$ [3]. In an ideal case, the range of $d(\mathbf{x})$ is $[0, +\infty)$, which makes the pixel values of $T(\mathbf{x})$ lies within the range $0 < T(\mathbf{x}) \le 1$.

$$I(\mathbf{x}) = J(\mathbf{x}), \text{ when } d(\mathbf{x}) \to 0, T(\mathbf{x}) \to 1 \tag{3}$$

(a) Haze Image   **(b)** $A_\infty^c = (255, 255, 255)$

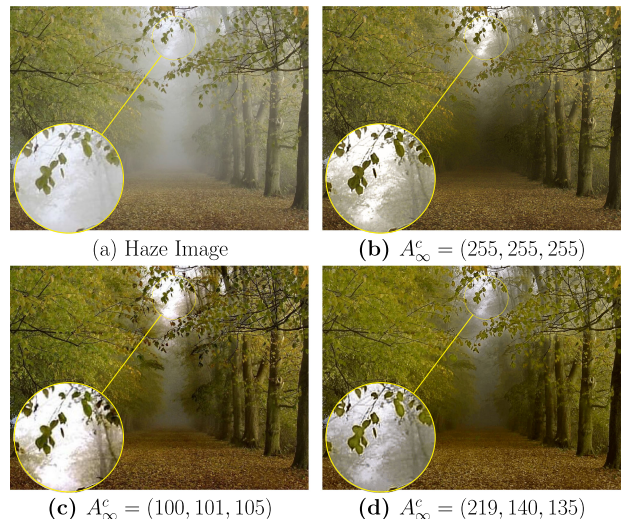**(c)** $A_\infty^c = (100, 101, 105)$ **(d)** $A_\infty^c = (219, 140, 135)$

Fig. 1. Significance of estimation of air-light (A_∞) in the dehazing framework. (a) Real haze image. (b) Impact of over-estimated A_∞ by He *et al.* [1], (c) Impact of under-estimated A_∞ impact by Berman *et al.* [6] (d) Accurately estimated A_∞ impact by our method.

Similarly,

$$I(\mathbf{x}) = A_\infty, \text{ when } d(\mathbf{x}) \to \infty, T(\mathbf{x}) \to 0 \tag{4}$$

In terrestrial imaging, Eq. (4) implies that the influence of air-light is stronger when a scenery object exists at a very large distance from the camera ($e^{-\beta d(x)} \approx 0$). Likewise, Eq. (3) implies that for shorter distance objects, the observed image is the actual scene radiance. However, in practical situations, both the ideal scenario given by Eq. (3) and Eq. (4) are not possible. Therefore, it becomes essential to investigate both A_∞ and $T(\mathbf{x})$ independently, to recover the haze-free image $J(x)$. Although extensive research has been done independently to estimate $T(\mathbf{x})$ using $d(\mathbf{x})$ [4]-[5], the task of estimating A_∞ is still considered in an ad-hoc manner. The importance of accurate A_∞ estimation is shown in Fig. 1 where the over-estimation of A_∞ causes darker dehazing results (see color of tree leaves and pathways in Fig. 1(b)), whereas due to the under-estimation of A_∞, microscopic details are lost from the bright fields (see Fig. 1(c)). In contrast, an accurate A_∞ estimation provides detailed dehazing effects (see Fig. 1(d)).

In earlier dehazing works [7]-[8], the brightest pixel value was usually interpreted as the global air-light vector. However, in practical situations, the selection of a pixel value from a

luminous object rather than a haze region for the air-light (A_∞) estimation often results in significant color distortion and loss of subtle detail. Later, He *et al*. [1] resolved this air-light estimation ambiguity by choosing the utmost 0.1% brightest pixels among the pixels of the dark channel. Tarel and Hautire *et al.* [3] neglects the existence of true air-light by selecting the pixel value [255, 255, 255] of pure white color as the global air-light vector. This method fails to estimate the ambient air-light in hazy scenes and often causes global darkness in dehazing results. In contrast, Meng *et al.* [9] uses the upmost pixel value of each RGB channel as the representative of global air-light. Sulami *et al.* [10] takes advantage of the Fattal color-line model [11] for the estimation of air-light magnitude and orientation. However, when distinct colors unable to form a line, the method fails to satisfy the assumption of the color-line model and causes extreme color-shifts. Inspired by the color-line model, Berman *et al.* [6] introduced the haze-line model for global air-light estimation. The model is utilizing the observation that pixels after blending with haze form a line pointing towards air-light, and their location could be estimated using the Hough transform in the RGB space. Although the method works well for estimating the global air-light vector using varying depth ranges, it is computationally intensive and often produces an over-exposed area in dehazing and causes loss of subtle details. Bahat and Irani [12] calculates the global air-light using the patch recurrence property. Zhu *et al.* [13] unites the color-line model and the haze-line model into the color-plane model for air-light estimation. The method uses RANSAC to approximate the air-light orientation and utilizing the global brightness assumption for magnitude estimation. The method is computationally intensive and causes an error when the assumptions are not satisfied.

II. BACKGROUND

In this section, we first describe a technique that is accepted by the majority of the researcher for air-light estimation.

A. Dark Channel Prior

The dark channel prior (DCP) [1] is widely used for global air-light (A_∞) estimation [4], [5], [15]. Mathematically, the dark channel of a hazy input $I(\mathbf{x})$ is defined using:

$$I^{dk}(\mathbf{x}) = \min_{\mathbf{y} \in \Omega(\mathbf{x})} \left(\min_{c \in \{r,g,b\}} I^c(\mathbf{y}) \right) \qquad (5)$$

where, I^c is the cth color-channel, Ω is an image local patch centered at pixel $\mathbf{x}$. By using DCP [1], the air-light (A_∞) contribution can be determined by selecting the upmost 0.1% of brightest pixels in the dark channel as:

$$A_\infty^c = I^c(arg \max_{\mathbf{x} \in P_{0.1\%}} \left(I^{dk}(\mathbf{x})\right)) \qquad (6)$$

In Eq. (6), among 0.1% of brightest pixels, the pixels corresponding to the utmost intensity in c^{th} color-channel of hazy input I are selected as the global air-light vector. Moreover, some variants of the air-light (A_∞) estimation modules has been in trend, but a majority of the dehazing works still rely either on DCP [1], user input, manual selection of a hazy-region or procedures [2], [9],

[10], [16], [17], where the intensity of any white or luminous scenery objects are often mistakenly chosen as air-light (A_∞) vector.

B. Limitations

Despite having effective dehazing performance, the DCP has some limitations:

1) Over-Estimation of Air-Light: The intensity of the luminous objects such as the lamps and sky is often mistakenly selected as A_∞, especially when scenery objects brighter than the haze exist. An impact of A_∞ over-estimation could be easily seen in Fig. 1(b), which causes underexposure and fails to bring out any significant detail even after dehazing.

2) Inefficient Estimation of Transmission-Map: On using DCP's Eq. (5) on Eq. (1), $T(\mathbf{x})$ can be derived as [18]:

$$T(\mathbf{x}) = 1 - w \left\{ \min_\Omega \left(\min_c \left(\frac{I^c(x)}{A_\infty^c} \right) \right) \right\} \qquad (7)$$

where $w(0 < w \le 1)$ is a constant parameter to preserve a tiny amount of haze for distant objects after dehazing [1]. In the haze, the local-color mixes with the air-light making it difficult to perceive the true colors. In such cases, Eq. (7) yields:

$$\min_\Omega \left(\min_c \left(\frac{I^c(x)}{A_\infty^c} \right) \right) \to 1 \quad \text{and } T(\mathbf{x}) \to 0 \qquad (8)$$

Eq. (8) implies, DCP fails to obtain $T(\mathbf{x})$ when the intensity of any luminous scenery object becomes similar to the A_∞.

III. PROPOSED METHODOLOGY

In this section, a novel statistical approach based on exploiting the haze impacts in different depth regions of an image is introduced for the air-light (A_∞) estimation.

A. Color Constancy Prior

The Color Constancy Prior (i.e., CCP) is based on the statistical observation that deeper-depth regions in an image can be regarded as the most haze-opaque. Although this observation has been widely accepted for $T(\mathbf{x})$ estimation [4]. The novelty of the proposed CCP is primarily to use this observation for A_∞ estimation rather than $T(\mathbf{x})$ estimation. The statistics to describe the haze impacts on color pixels located at different scene-depth are shown in Fig. 2. It can be seen from the average histograms drawn for each close-up patch in Fig. 2(b) that pixels brightness (i.e., air-light effect) is pretty low in the regions of shallow-depth and the image local details are usually with vivid colors. But as the scene-depth increases, the haze contribution also increases, which in turn escalates the brightness of the pixels in distant areas and making it difficult to perceive the real colors of the scene. Furthermore, it can also be confirmed from the air-light (A_∞) profile shown in Fig. 2(c) that A_∞ contribution rapidly varies with the scene-depth $d(\mathbf{x})$ and attains a highest value for the distant scenery object. Therefore, inspired by such experimental observation, it can be said that in deeper-depth region, the actual color of the pixel escalates towards the higher intensity side becomes the most haze-opaque and
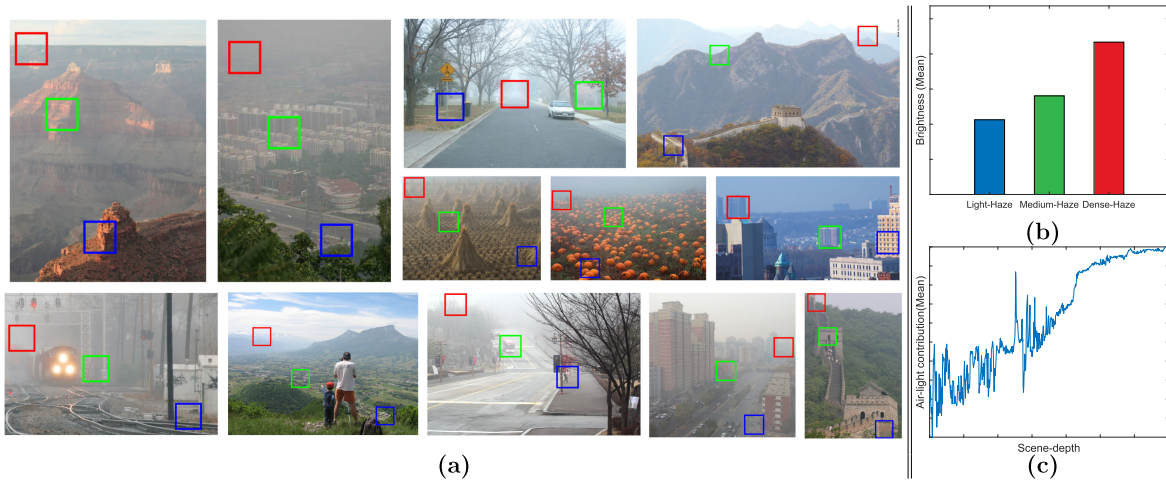
Fig. 2. Pictorial illustrations to represent the haze impacts in different regions of an image. (a) Original haze images with manually identified light-haze, medium-haze, and dense-haze regions [14]. (b) Average histogram of all haze-regions. (c) The air-light profile along the scene-depth (Note: the brightness mean in Fig. 2(b) is generated from 4000 manually extracted 71×71 close-up patches, whereas in Fig. 2(c) the air-light profile is generated from 400 real haze images).

contains a reasonable amount of air-light (A_∞). This statistical observation, to describe the A_∞ distribution in haze images is named as color constancy prior because the apparent color in the deeper-depth or haze-opaque region remains constant despite changes in the intensity and spectral composition of the haze illumination. Additionally, it can be seen from Fig. 2(c) that the average amount of air-light present in the dense haze region is much higher than in the low and medium haze regions, which effectively saturates the background colors and causes negligible variation in its intensity (slope of the intensity variation curve tends to zero) compared to other areas and introduce a character of constancy. Mathematically, the CCP is derived using the following steps:

$$h_i = \min_{\mathbf{y} \in \Omega_i(\mathbf{x_i})} I_{hsv}^v(\mathbf{y}) \tag{9}$$

where "v" is the escalated pixel brightness in the HSV color space. To find A_∞, first sort the unordered collection of pixel elements in vector $H = \{h_i\}_{i=1}^{\mathbb{N}}, (\mathbb{N} = M \times N)$ in descending order. Since H is a finite length vector after $\mathbb{N}$-steps, we get an ordered sequence of elements S_1 as:

$$S_1 = [h_1^\star, h_2^\star, h_3^\star, \dots h_{\mathbb{N}}^\star] \tag{10}$$

where $h_1^\star = \max\{H\}, h_{\mathbb{N}}^\star = \min\{H\}$. After sorting S_1, upper $\alpha_\%$ of pixels are identified as the brightest pixels (K_B):

$$K_B = I_{hsv}^v(L_1) = \{k_{B1}, k_{B2}, k_{B3}, \dots k_{B\mathbb{M}}\} \tag{11}$$

where $\mathbb{M} < \mathbb{N}, L_1 = \{i \mid h_i \geq h_{\frac{\mathbb{N}}{\alpha}}^\star\}$ is the index of α brightest pixels. Among K_B, there might be few pixels corresponding to the most luminous scenery object, which may cause wrong-estimation of A_∞. Therefore, to solve this problem, the brightest pixel set (K_B) is sorted in descending order:

$$S_2 = [k_{B_1}^\star, k_{B_2}^\star, k_{B_3}^\star, \dots k_{B_{\mathbb{M}}}^\star] \tag{12}$$

where $k_{B_1}^\star = \max\{K_B\}, k_{B_{\mathbb{M}}}^\star = \min\{K_B\}$. After sorting S_2, the primary $\gamma_\%$ of pixels corresponding to the brightest ones are

ignored to identify the brighter pixels set (K_b):

$$K_b = I_{hsv}^v(L_2) = \{k_{b1}, k_{b2}, k_{b3}, \dots k_{b\mathbb{M}'}\} \tag{13}$$

where $\mathbb{M}' < \mathbb{M}, L_2 = \{j \mid k_{B_j}^\star < k_{B\frac{\mathbb{M}}{\gamma}}^\star\}$ is the index of brighter pixels. Once, we obtained the indices of the brighter pixels, the global air-light vector A_∞ can be estimated using:

$$A_\infty = I\left[mod(F, M), \lceil \frac{F}{M} \rceil\right] \tag{14}$$

where $F = \min\{L_4\}, L_4 = \{L_1(j) \mid j \in L_3\}$, and $L_3 = \{j \mid K_{b_j} = \max(K_b)\}$. In the definition of L_3, an index with a pixel value equal to the maximum value of the brighter pixel set (K_b) is chosen as the haziest pixel index (L_3), which may have one or several values. Here, in the definition of L_4, the haziest pixel index (L_3) is used for L_1 so that their index is effectively searched between the indexes of the main pixels. Among L_4, there might be many possible indices of the haziest pixel, so the closest index can be chosen using $F = \min\{L_4\}$. In Eq. (14), $mod(F, M)$ and $\lceil \frac{F}{M} \rceil$ are used to retrieve the location of the most haze-opaque pixels in the input image I.

IV. EVALUATION AND RESULTS

This section presents an assessment of the proposed method on a variety of terrestrial and underwater haze images, obtained from well-known LIVE databases [14], UIEB dataset [19], and other authors' letters [12]. To validate the performance, a subjective study has been performed on 50 participants using the Bradley-Terry model [20] to manually identify the GT of air-light (A_∞) from the most haze-opaque region. After some extensive experiments, the parameters are set to $\alpha = 10$ and $\gamma = 0.4$ for optimal results. An example of global air-light (A_∞) estimation for different types of haze images is shown in Fig. 3. Upon zooming the estimated air-light pixel clusters in Fig. 3(b), it can be seen that He *et al.* [1], Meng *et al.* [9], and Bahat *et al.* [12] methods often selects the brightest region intensity as the global air-light, whereas the Berman *et al.* [6] method is
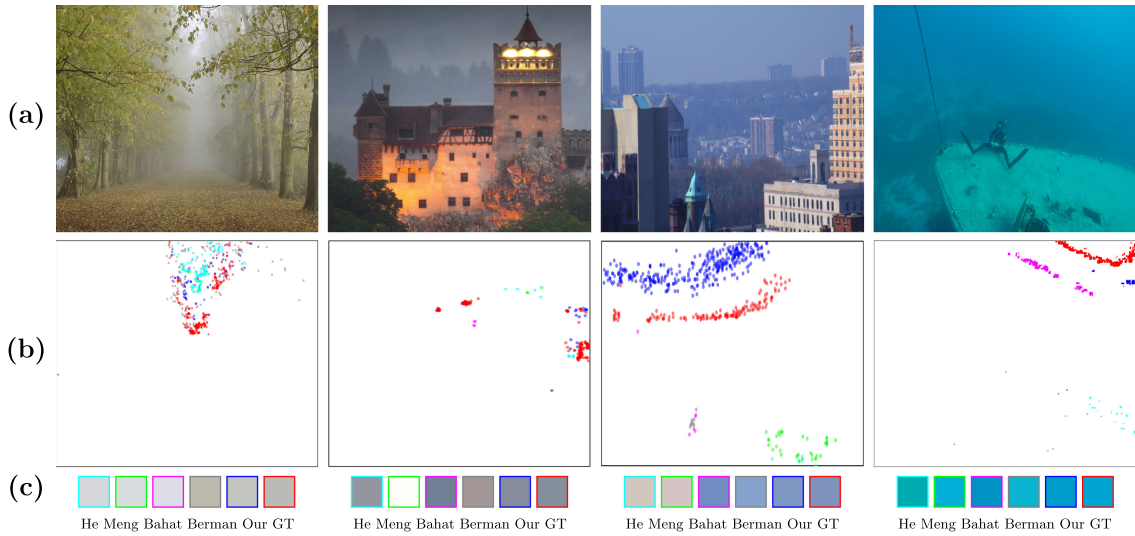
Fig. 3.   An example of global air-light (A_∞) estimation with other state-of-the-art methods. (a) Real haze images. (b) The air-light (A_∞) pixel clusters, where each color represents A_∞ estimated by different methods. (c) The air-light (A_∞) color estimated by He *et al.* [1], Meng *et al.* [9], Bahat *et al.* [12], Berman *et al.* [6] and ours along with manually identified GT.
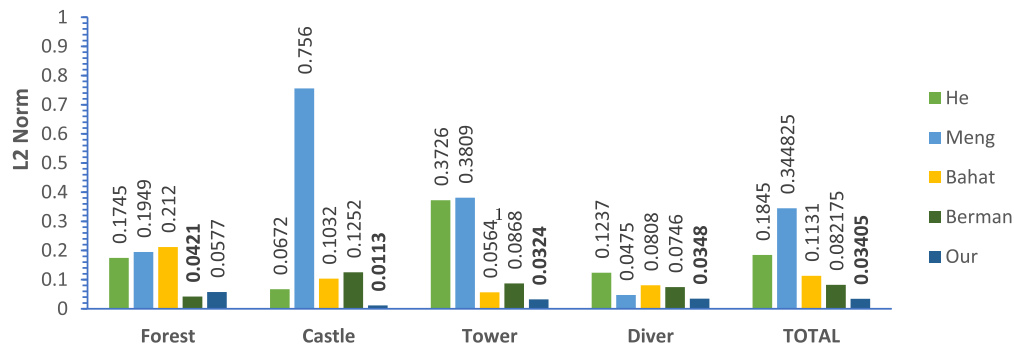

Fig. 4.   Accuracy evaluation of global air-light (A_∞) estimation in terms of L2-norm.

somewhat successful in obtaining A_∞ from the haze-regions (see the second and third images from the left, the method fails and incorrectly selects the intensity of the rock and the dome as the air-light (A_∞). Unlike other methods, the proposed CCP shows consistent performance by obtaining A_∞ from the most haze-opaque areas only. Notably, the proposed CCP is intended to retrieve only A_∞ so that it could be used efficiently in Eq. (1) for $J(\mathbf{x})$ retrieval. Therefore, to quantitatively measure the relative error, a classic metric namely L2-norm has been used. As can be seen from experimental validation in Fig. 4, the proposed CCP can consistently estimate A_∞ closer to GT even when luminous scenery objects and unwanted color-cast exist. (see supplementary material for CCP dehazing performance).

A. Complexity Analysis

Time complexity of an algorithm is a direct measure of its efficiency. In the proposed method computational cost is bounded on the higher side by three main operations, namely, statistical filtering operation, the sorting operation, and updation

of intermediate variables. The statistical filtering operations requires $O(N)$ complexity through an intelligent sliding window approach [21]. The sorting operation requires $O(N log N)$ operations and updation of intermediate variables is bound at $O(N)$ respectively. Therefore, the overall complexity of our method is $O(N log N)$.

V. CONCLUSION

In this letter, the problem of air-light estimation in single haze images is addressed and proposed a theoretically well-grounded color constancy prior (CCP) for their retrieval. The CCP is inspired by the statistical observation that in distant scenery objects, the true color of a pixel becomes the most haze-opaque. The CCP is simple, fast, and can easily retrieve the air-light (A_∞) even under considerable variation in illumination. Experimental results on a variety of haze images demonstrate that the proposed CCP is effective and performs better than other state-of-the-art air-light recovery methods. In future work, we intend to examine the performance of CCP on sandstorm images influenced by severe color-cast.

REFERENCES

[1] K. He, J. Sun, and X. Tang, "Single image haze removal using dark channel prior," *IEEE Trans. Pattern Anal. Mach. Intell.*, vol. 33, no. 12, pp. 2341–2353, Dec. 2011.

[2] D. Berman, T. Treibitz, and S. Avidan, "Air-light estimation using haze-lines," in *Proc. IEEE Int. Conf. Comput. Photography (ICCP)*, May 2017, pp. 1–9.

[3] J.-P. Tarel and N. Hautière, "Fast visibility restoration from a single color or gray level image," in *Proc. IEEE Int. Conf. Comput. Vis. (ICCV'09)*, Kyoto, Japan, 2009, pp. 2201–2208. [Online]. Available: http://perso.lcpc.fr/tarel.jean-philippe/publis/iccv09.html

[4] Q. Zhu, J. Mai, and L. Shao, "A fast single image haze removal algorithm using color attenuation prior," *IEEE Trans. Image Process.*, vol. 24, no. 11, pp. 3522–3533, Nov. 2015.

[5] B. Cai, X. Xu, K. Jia, C. Qing, and D. Tao, "DehazeNet: An end-to-end system for single image haze removal," *IEEE Trans. Image Process.*, vol. 25, no. 11, pp. 5187–5198, Nov. 2016.

[6] D. Berman, T. Treibitz, and S. Avidan, "Non-local image dehazing," in *Proc. IEEE Conf. Comput. Vis. Pattern Recognit. (CVPR)*, Jun. 2016, pp. 1674–1682.

[7] R. T. Tan, "Visibility in bad weather from a single image," in *Proc. IEEE Conf. Comput. Vis. Pattern Recognit.*, Jun. 2008, pp. 1–8.

[8] R. Fattal, "Single image dehazing," *ACM Trans. Graph.*, vol. 27, no. 3, pp. 1–9, Aug. 2008. [Online]. Available: https://doi.org/10.1145/1360612.1360671

[9] G. Meng, Y. Wang, J. Duan, S. Xiang, and C. Pan, "Efficient image dehazing with boundary constraint and contextual regularization," in *Proc. IEEE Int. Conf. Comput. Vis.*, Dec. 2013, pp. 617–624.

[10] M. Sulami, I. Glatzer, R. Fattal, and M. Werman, "Automatic recovery of the atmospheric light in hazy images," in *Proc. IEEE Int. Conf. Comput. Photography (ICCP)*, May 2014, pp. 1–11.

[11] R. Fattal, "Dehazing using color-lines," *ACM Trans. Graph.*, vol. 34, no. 1, pp. 13:1–13:14, Dec. 2014. [Online]. Available: http://doi.acm.org/10.1145/2651362

[12] Y. Bahat and M. Irani, "Blind dehazing using internal patch recurrence," in *Proc. IEEE Int. Conf. Comput. Photography (ICCP)*, May 2016, pp. 1–9.

[13] M.-Z. Zhu, B.-W. He, and L.-W. Zhang, "Atmospheric light estimation in hazy images based on color-plane model," *Comput. Vis. Image Understanding*, vol. 165, pp. 32–42, 2017.

[14] L. K. Choi, J. You, and A. C. Bovik, "Referenceless prediction of perceptual fog density and perceptual image defogging," *IEEE Trans. Image Process.*, vol. 24, no. 11, pp. 3888–3901, Nov. 2015.

[15] D. Yang and J. Sun, "Proximal dehaze-Net: A prior learning-based deep network for single image dehazing," in *Proc. ECCV*, 2018, pp. 729–746.

[16] M.-Z. Zhu, B.-W. He, and L.-W. Zhang, "Atmospheric light estimation in hazy images based on color-plane model," *Comput. Vis. Image Understanding*, vol. 165, pp. 33–42, 2017. [Online]. Available: http://www.sciencedirect.com/science/article/pii/S1077314217301637

[17] L. Shi, B. Chen, S. Huang, A. O. Larin, O. S. Seredin, A. V. Kopylov, and S. Kuo, "Removing haze particles from single image via exponential inference with support vector data description," *IEEE Trans. Multimedia*, vol. 20, no. 9, pp. 2503–2512, Sep. 2018.

[18] S. Gautam, T. K. Gandhi, and B. K. panigrahi, "Single image dehazing using image boundary constraint and nearest neighborhood optimization," in *Proc. 11th Indian Conf. Comput. Vis., Graph. Image Process.*, Hyderabad, India, 2018, p. 5.

[19] C. Li, C. Guo, W. Ren, R. Cong, J. Hou, S. Kwong, and D. Tao, "An underwater image enhancement benchmark dataset and beyond," *IEEE Trans. Image Process.*, vol. 29, pp. 4376–4389, 2020.

[20] O. Dykstra, "Rank analysis of incomplete block designs: A method of paired comparisons employing unequal repetitions on pairs," *Biometrics*, vol. 16, no. 2, pp. 176–188, 1960. [Online]. Available: http://www.jstor.org/stable/2527550

[21] T. Huang, G. Yang, and G. Tang, "A fast two-dimensional median filtering algorithm," *IEEE Trans. Acoust., Speech, Signal Process.*, vol. ASSP-27, no. 1, pp. 13–18, 1979.